Ring-Closing Metathesis of Olefinic Peptides: Design, Synthesis, and Structural Characterization of Macrocyclic Helical Peptides

Helen E. Blackwell,[†,‡] Jack D. Sadowsky,[§] Rebecca J. Howard,[§] Joshua N. Sampson,[§] Jeffery A. Chao,[§] Wayne E. Steinmetz,[§] Daniel J. O'Leary,*[,§] and Robert H. Grubbs*[,†]

The Arnold and Mabel Beckman Laboratory of Chemical Synthesis, Division of Chemistry and Chemical Engineering, California Institute of Technology, Pasadena, California 91125, and Department of Chemistry, Pomona College, Claremont, California 91711

doleary@pomona.edu

Received January 20, 2001

Heptapeptides containing residues with terminal olefin-derivatized side chains (**3** and **4**) have been treated with ruthenium alkylidene **1** and undergone facile ring-closing olefin metathesis (RCM) to give 21- and 23-membered macrocyclic peptides (**5** and **6**). The primary structures of peptides **3** and **4** were based upon a previously studied heptapeptide (**2**), which was shown to adopt a predominantly 3_{10}-helical conformation in $CDCl_3$ solution and an α-helical conformation in the solid state. Circular dichroism, IR, and solution-phase ^1H NMR studies strongly suggested that acyclic precursors **3** and **4** and the fully saturated macrocyclic products **7** and **8** also adopted helical conformations in apolar organic solvents. Single-crystal X-ray diffraction of cyclic peptide **8** showed it to exist as a right-handed 3_{10}-helix up to the fifth residue. Solution-phase NMR structures of both acyclic peptide **4** and cyclic peptide **8** in CD_2Cl_2 indicated that the acyclic diene assumes a loosely 3_{10}-helical conformation, which is considerably rigidified upon macrocyclization. The relative ease of introducing carbon−carbon bonds into peptide secondary structures by RCM and the predicted metabolic stability of these bonds renders olefin metathesis an exceptional methodology for the synthesis of rigidified peptide architectures.

Introduction

Due to the frequency of helical secondary structures in peptides and proteins, considerable effort has been directed toward the design of small molecule helix mimetics and stabilized helical structures.[1,2] For example, designed organic template molecules that initiate α-helix formation in peptide sequences have been reported by Kemp et al.[3] Oligomers of certain *β*-amino acids (*β*-peptides) have matured into a promising class of helical peptide analogues.[4] Short α-helical peptides have been rigidified by incorporation of naturally occurring capping motifs[5] and by stabilization of the intrinsic helix dipole.[6] Notably, significant progress has been made toward stabilizing small, synthetic helical peptides through the incorporation of covalent or noncovalent linkages between constituent amino acid side chains. Examples include salt bridges,[7] lactams,[8] disulfide bridges,[9] hydrophobic effects,[10] and metal ligation between natural[11] and unnatural amino acids.[12] Substantial helix stabilization has been achieved when the tether was positioned between the (*i*) and either ($i + 4$) or ($i + 7$) residues in the peptide backbone. Such a linkage encompasses approximately one or two turns of an α-helical peptide backbone and places the tethered side chains on the same side of the helix.

* Address all correspondence to D.J.O.
† California Institute of Technology.
‡ Current address: Department of Chemistry and Chemical Biology, Harvard University, Cambridge, MA 02138.
§ Pomona College.

(1) For preliminary accounts of this work, see: (a) Blackwell, H. E.; Grubbs, R. H. *Angew. Chem., Int. Ed. Engl.* **1998**, *37*, 3281−3284. (b) Blackwell, H. E. Ph.D. Thesis, California Institute of Technology, 1999.

(2) The α-helical conformation is adopted by 40% of all residues in proteins. See: Creighton, T. E. *Proteins: Structures and Molecular Properties*, 2nd ed.; Freeman: New York, 1984; pp 182−188.

(3) Kemp, D. S.; Curran, T. P.; Boyd, J. G.; Allen, T. J. *J. Org. Chem.* **1991**, *56*, 6683−6697, and references therein.

(4) For representative examples of helical *β*-peptides, see: (a) Seebach, D.; Ciceri, P. E.; Overhand, M.; Jaun, B.; Rigo, D.; Oberer, L.; Hommel, U.; Amstutz, R.; Widmer, H. *Helv. Chim. Acta* **1996**, *79*, 2043−2066. (b) Seebach, D.; Matthew, J. L. *Chem. Commun.* **1997**, 2015−2022. (c) Sifferlen, T.; Rueping, M.; Gademann, K.; Jaun, B.; Seebach, D. *Helv. Chim. Acta* **1999**, *82*, 2067−2093. (d) Appella, D. H.; Christianson, L. A.; Karle, I. L.; Powell, D. R.; Gellman, S. H. *J. Am. Chem. Soc.* **1999**, *121*, 6206−6212. (e) Appella, D. H.; Durell, S. R.; Barchi, J. J.; Gellman, S. H. *J. Am. Chem. Soc.* **1999**, *121*, 2309−2310. (f) Hamuro, Y.; Schneider, J. P.; DeGrado, W. F. *J. Am. Chem. Soc.* **1999**, *121*, 12200−12201.

(5) (a) Forood, B.; Feliciano, E. J.; Nambiar, K. P. *Proc. Natl. Acad. Sci. U.S.A.* **1994**, *90*, 838−842. (b) Zhou, H. X.; Lyu, P. C.; Wemmer, D. E.; Kallenbach, N. R. *J. Am. Chem. Soc.* **1994**, *116*, 1139−1140.

(6) Schoemaker, K. R.; Kim, P. S.; York, E. J.; Stewart, J. M.; Baldwin, R. L. *Nature* **1987**, *326*, 563−567.

(7) Scholtz, J. M.; Qian, H.; Robbins, V. H.; Baldwin, R. L. *Biochemistry* **1993**, *32*, 9668−9676 and references therein.

(8) Phelan, J. C.; Skelton, N. J.; Braisted, A. C.; McDowell, R. S. *J. Am. Chem. Soc.* **1997**, *119*, 455−460 and references therein.

(9) (a) Jackson, D. Y.; King, D. S.; Chmielewski, J.; Singh, S.; Schultz, P. G. *J. Am. Chem. Soc.* **1991**, *113*, 9391−9392. (b) For an example of a helical *β*-peptide stabilized by an intramolecular disulfide, see: Rueping, M.; Jaun, B.; Seebach, D. *J. Chem. Soc., Chem. Commun.* **2000**, 2267−2268.

(10) Albert, J. S.; Hamilton, A. D. *J. Am. Chem. Soc.* **1995**, *34*, 984−990.

(11) (a) Ghadiri, M. R.; Fernholz, A. K. *J. Am. Chem. Soc.* **1990**, *112*, 9633−9635. (b) Todd, R. J.; Van Dam, M. E.; Casimiro, D.; Haymore, B. L.; Arnold, F. H. *Proteins: Struct., Funct., Genet.* **1991**, *10*, 156−161. (c) Kelso, M. J.; Hoang, H. N.; Appleton, T. G.; Fairlie, D. P. *J. Am. Chem. Soc.* **2000**, *122*, 10488−10489.

(12) (a) Ruan, F.; Chen, Y.; Hopkins, P. B. *J. Am. Chem. Soc.* **1990**, *112*, 9403−9404. (b) Gilbertson, S. R.; Wang, X. *J. Org. Chem.* **1996**, *61*, 434−435.

10.1021/jo015533k CCC: $20.00
Published on Web 05/11/2001

The exceptional functional group tolerance of the olefin metathesis catalyst $(PCy_3)_2Cl_2Ru{=}CHPh$ (**1**)[13] has enabled the synthesis of cyclic amino acids[14] and peptides[15] exhibiting β-turn[16] and β-sheet[17] secondary structures via ring-closing olefin metathesis (RCM).[18−20] This transformation effectively introduces non-native carbon−carbon bond constraints, which can afford enhanced biostability in peptides and proteins and induce unique secondary structural motifs.[21] The intrinsic power of RCM in the synthesis of constrained cyclic peptides was recently demonstrated by Liskamp and co-workers, where two terminal olefin moieties were moved sequentially to each amide NH along the Leu-enkephalin peptide backbone and subjected to RCM to generate all permutations of the possible cyclic products.[15e] We previously communicated the concise synthesis of macrocyclic 3_{10}-helical peptides via the RCM of olefin-derivatized amino acid residues at the (*i*) and (i + 4) positions in the peptide backbone.[1a] Recently, Verdine and co-workers have also introduced all-carbon cross-links into peptide helices at the (*i*) and (i + 4) or (i + 7) positions via a similar RCM strategy, yielding macrocyclic peptides with both increased helix stability and concurrent resistance to certain cellular proteases.[22] In this paper, we present the full details of the design, synthesis, and structural analyses of a set macrocyclic helical peptides, wherein RCM is employed to incorporate a C−C tether between strategically positioned amino acid side chains.

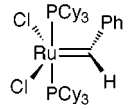

1

Selection of a Model Heptapeptide Helix. We chose to study hydrophobic peptide model systems from the outset, partly because the use of apolar amino acid sequences permits characterization of conformation in poorly solvating organic solvents.[23] Furthermore, ruthenium alkylidene **1** exhibits its highest metathesis activity in these media.[24] We became interested in a hydrophobic, organic-soluble heptapeptide (**2**) studied by Karle and Balaram et al.,[25] which contains two repeat units of valine-alanine-leucine (Val-Ala-Leu) separated by one α-aminoisobutyric acid residue (Aib) (Figure 1).

2 = Boc-Val-**Ala**-Leu-Aib-Val-**Ala**-Leu-OMe
3-4 = Boc-Val-**X**-Leu-Aib-Val-**X**-Leu-OMe

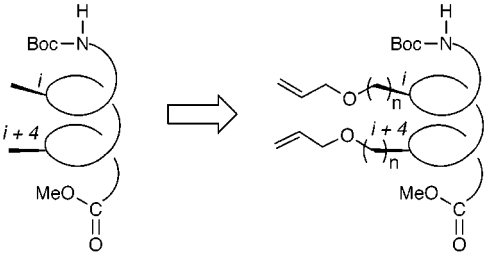

2 **3**: X = Ser (n = 1)
4: X = Hse (n = 2)

Figure 1. Karle and Balaram's heptapeptide **2** and two dienic analogues **3** and **4**.

The Aib residue is well-known to stabilize 3_{10}- and/or α-helical conformations in apolar oligopeptides and is frequently found in peptides produced by microbial sources.[26] Examples of such Aib-rich peptides include the antibiotics zervamicin, alamethicin, and trichogin A IV, which are believed to adopt helical conformations within lipid bilayer membranes and aggregate therein to form ion channels. Heptapeptide **2** was shown to adopt a predominantly α-helical conformation in the solid state by X-ray crystallography and was found to adopt the structurally related 3_{10}-helical conformation in $CDCl_3$ by solution-phase ^1H NMR analyses.[25] Encouraged by these

(13) PCy_3 = tricyclohexylphosphine. For the synthesis and characterization of catalyst **1**, see: (a) Schwab, P.; France, M. B.; Ziller, J. W.; Grubbs, R. H. *Angew. Chem., Int. Ed. Engl.* **1995**, *34*, 2039−2041. (b) Schwab, P.; Grubbs, R. H.; Ziller, J. W. *J. Am. Chem. Soc.* **1996**, *118*, 100−110. (c) Belderrain, T. R.; Grubbs, R. H. *Organometallics* **1997**, *16*, 4001−4003.

(14) (a) Miller, S. J.; Grubbs, R. H. *J. Am. Chem. Soc.* **1995**, *117*, 5855−5856. (b) Rutjes, F. P. J. T.; Schoemaker, H. E. *Tetrahedron Lett.* **1997**, *48*, 677−680. (c) Hammer, K.; Undheim, K. *Tetrahedron* **1997**, *53*, 2309−2322. (d) Campagne, J.-M.; Ghosez, L. *Tetrahedron Lett.* **1998**, *39*, 6175−6178. (e) Sauriat-Dorizon, H.; Guibé, F. *Tetrahedron Lett.* **1998**, *39*, 6711−6714. (f) Kotha, S.; Sreenivasachary, N. *Biorg. Med. Chem. Lett.* **1998**, *8*, 257−260. (g) Kotha, S.; Sreenivasachary, N.; Brahmachary, E. *Tetrahedron Lett.* **1998**, *39*, 2805−2808. (h) Osipov, S. N.; Bruneau, C.; Picquet, M.; Kolomiets, A. F.; Dixneuf, P. H. *J. Chem. Soc., Chem. Commun.* **1998**, 2053−2054. (i) Tjen, K. C. M. F.; Kinderman, S. S.; Schoemaker, H. E.; Hiemstra, H.; Rutjes, F. P. J. T. *J. Chem. Soc., Chem. Commun.* **2000**, 699−700.

(15) For examples of cyclic peptides prepared via RCM that do not adopt specific secondary structural conformations, see: (a) ref 14a. (b) O'Leary, D. J.; Miller, S. J.; Grubbs, R. H. *Tetrahedron Lett.* **1998**, *39*, 1689−1690. (c) Ripka, A. S.; Bohacek, R. S.; Rich, D. H. *Bioorg. Med. Chem. Lett.* **1998**, *8*, 357−360. (d) Kazmaier, U.; Maier, S. *Org. Lett.* **1999**, *1*, 1763−1766. (e) Reichwein, J. F.; Wels, B.; Kruijtzer, J. A. W.; Versluis, C.; Liskamp, R. M. J. *Angew. Chem., Int. Ed. Engl.* **1999**, *38*, 3684−3687. (f) Reichwein, J. F.; Versluis, C.; Liskamp, R. M. J. *J. Org. Chem.* **2000**, *65*, 6187−6195.

(16) (a) Miller, S. J.; Blackwell, H. E.; Grubbs, R. H. *J. Am. Chem. Soc.* **1996**, *118*, 9606−9614. (b) Pernerstorfer, J.; Schuster, M.; Blechert, S. *J. Chem. Soc., Chem. Commun.* **1997**, 1949−1950. (c) Fink, B. E.; Kym, P. R.; Katzenellenbogen, J. A. *J. Am. Chem. Soc.* **1998**, *120*, 4334−4344. (d) For an example of a macrocyclic octapeptide β-hairpin, see: Jarvo, E. R.; Copeland, G. T.; Papaioannou, N.; Bonitatebus, P. J.; Miller, S. J. *J. Am. Chem. Soc.* **1999**, *121*, 11638−11643.

(17) (a) Clark, T. D.; Ghadiri, M. R. *J. Am. Chem. Soc.* **1995**, *117*, 12364−12365. (b) Clark, T. D.; Kobayashi, K.; Ghadiri, M. R. *Chem. Eur. J.* **1999**, *5*, 782−792.

(18) For recent reviews of RCM in organic synthesis, see: (a) Schuster, M.; Blechert, S. *Angew. Chem., Int. Ed. Engl.* **1997**, *36*, 2036−2056. (b) Grubbs, R. H.; Chang, S. *Tetrahedron* **1998**, *54*, 4413−4450. (c) Fürstner, A. *Angew. Chem., Int. Ed.* **2000**, *39*, 3012−3043.

(19) For examples of the synthesis of *linear* amino acid and peptide derivatives by olefin cross-metathesis employing **1**, see: (a) Feng, J.; Schuster, M.; Blechert, S. *Synlett* **1997**, 129−130. (b) Schuster, M.; Lucas, N.; Blechert, S. *J. Chem. Soc., Chem. Commun.* **1997**, 823−824. (c) Gibson, S. E.,; Gibson, V. C.; Keen, S. P. *J. Chem. Soc., Chem. Commun.* **1997**, 1107−1108. (d) Baigini, S. C. G.; Gibson, S. E.; Keen, S. P. *J. Chem. Soc., Perkin Trans. 1* **1998**, *16*, 2485−2499. (e) Blackwell, H. E.; O'Leary, D. J.; Chatterjee, A. K.; Washenfelder, R. A.; Bussmann, D. A.; Grubbs, R. H. *J. Am. Chem. Soc.* **2000**, *122*, 58−71. (f) For the synthesis of an amino acid derivative by yne-ene cross-metathesis, see: Schuster, M.; Blechert, S. *Tetrahedron Lett.* **1998**, *39*, 2295−2298.

(20) For a recent review of transition metal-mediated organic synthesis, see: Hegedus, L. S. *Coord. Chem. Rev.* **2000**, *204*, 199−307.

(21) For a recent nonmetathesis approach for the introduction of aliphatic linkages into peptides, see: (a) Andrews, M. J. I.; Tabor, A. B. *Tetrahedron Lett.* **1997**, *38*, 3063−3066. (b) McNamara, L. M. A.; Andrews, M. J. I.; Mitzel, F.; Siligardi, G.; Tabor, A. B. *Tetrahedron Lett.* **2001**, *42*, 1591−1593.

(22) Schafmeister, C. E.; Po, J.; Verdine, G. L. *J. Am. Chem. Soc.* **2000**, *122*, 5891−5892.

(23) Karle, I. L.; Balaram, P. *Biochemistry* **1990**, *29*, 6747−6756.

(24) Benzylidene **1** is soluble and most active in CH_2Cl_2, $CHCl_3$, and C_6H_6.

(25) (a) Karle, I. L.; Flippen-Anderson, J. L.; Uma, K.; Balaram, P. *Proteins: Struct., Funct., Genet.* **1990**, *7*, 62−73. (b) Karle, I. L.; Flippen-Anderson, J. L.; Uma, K.; Balaram, P. *Biopolymers* **1993**, *33*, 827−837.

(26) For general reviews on Aib containing peptides, see: (a) ref 23. (b) Toniolo, C.; Benedetti, E. *Macromolecules* **1991**, *24*, 4004−4009. (c) Karle, I. L. *Biopolymers* **1996**, *40*, 157−180. (d) Karle, I. *Acc. Chem. Res.* **1999**, *32*, 693−701.

Scheme 1. Synthesis of Peptide Macrocycles via a Two-Step RCM and Hydrogenation Procedure[a]

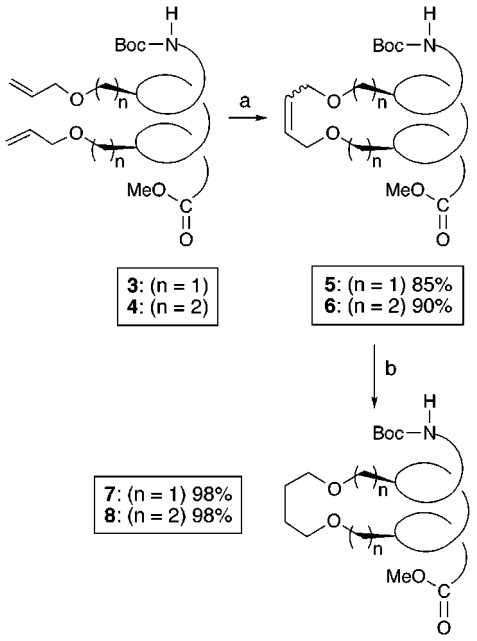

[a] Key: (a) 20 mol % **1**, $CHCl_3$, 25 °C; (b) cat. 10% Pd−C, 1 atm H_2, EtOH, 25 °C.

structural results, we chose to use heptapeptide **2** as a scaffold upon which to build acyclic peptide dienes.

Results and Discussion

Synthesis of Cyclic Heptapeptides via RCM. Through analysis of the X-ray structure of model peptide **2** and molecular modeling, we predicted that replacement of the (*i*) and (*i* + 4) Ala residues of **2** with residues containing side-chain terminal olefin groups would place the two olefins in proximity to one another, provided that our dienic analogues also adopted an α-helical conformation and that the derivatized side chains were of an appropriate length. L-Serine (Ser) and L-homoserine (Hse) *O*-allyl ethers were selected as olefin-containing residues, due to their ready availability and straightforward derivatization as allyl ethers.[27] Acyclic peptide dienes **3** and **4**, shown schematically in Figure 1, were then prepared by standard solution-phase peptide chemistry.[28]

Dienes **3** and **4** were each treated with alkylidene **1** (20 mol % **1**, 5 mM in **3** or **4**, $CHCl_3$, 25 °C, 3−4 h) to yield 21- and 23-membered macrocyclic alkenes **5** and **6** in 85% and 90% yields, respectively (Scheme 1).[29] Each macrocycle was isolated as a mixture of olefin isomers (ca. 5:1 *E*/*Z*).[30] Both RCM reactions appeared quantitative by thin-layer chromatography (TLC) analyses; the reduced yield is due only to isolation by column chromatography on silica gel. Subsequent catalytic hydrogenation (10% Pd−C, 1 atm H_2, EtOH, 25 °C, 2 h) afforded the saturated species **7** and **8** in excellent yields. The high yield, the relatively fast rate of the RCM transformation, and the lack of competing intermolecular cross-metathesis suggested that the acyclic dienes were preorganized for ring closure in organic solvents. This prompted closer examination of the structures of acyclic peptides **3** and **4**, along with cyclic products **7** and **8**.

Table 1. IR Amide NH Bands for Acyclic and Cyclic Heptapeptides (1.0 mM in $CHCl_3$, 25 °C)

peptide	3	4	7	8
non-H-bonded NH band (cm^{-1})	3428	3438	3431	3426
H-bonded NH band (cm^{-1})	3323	3325	3331	3325

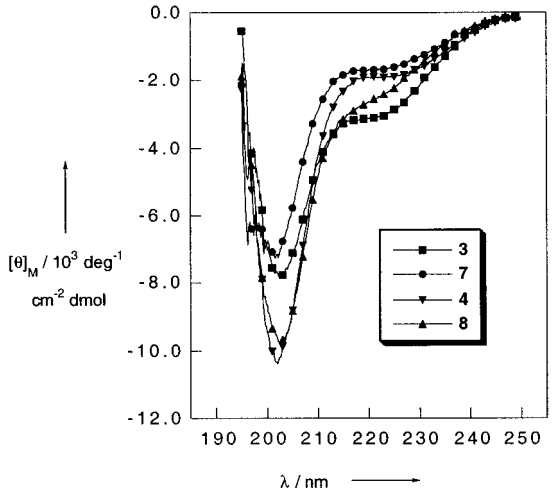

Figure 2. CD spectra (250−195 nm) of peptides **3**, **4**, **7**, and **8** (1 mM) in TFE at 25 °C. Total molar ellipticity values are given.

IR and CD Studies of the Acyclic and Cyclic Peptides. Table 1 lists the amide NH region of the IR spectra of the heptapeptides **3**, **4**, **7**, and **8** in $CHCl_3$ solutions (1.0 mM, 25 °C). In each case, the characteristic bands for both non-hydrogen-bonded NH groups (>3400 cm^{-1}) and intramolecular C═O···H−N hydrogen bonds appear (<3400 cm^{-1}).[31] Notably, the latter bands were considerably stronger than the former, indicating that the majority of the amide NHs in structures **3**, **4**, **7**, and **8** are involved in intramolecular H-bonds in dilute $CHCl_3$ solutions (approximating the RCM reaction conditions). Although it is impossible to establish from the IR data alone which of the amide NH groups are involved in intramolecular H-bonding, these data are consistent with the possibility of extensive transannular intramolecular H-bonding in both the acyclic (**3** and **4**) and cyclic structures (**7** and **8**), suggesting that helical conformations could be adopted in $CHCl_3$.

Further qualitative measurements of the conformation of the heptapeptides were obtained by far-UV circular dichroism (CD). CD spectra of solutions of peptides **3**, **4**, **7**, and **8** in trifluoroethanol (TFE) at 25 °C are shown in Figure 2. For peptides and proteins, TFE has been shown to be a strongly helix promoting solvent comparable to

(27) Sugano, H.; Miyoshi, M. *J. Org. Chem.* **1976**, *41*, 2352−2353.

(28) All L-amino acids were used. See: Bodansky, M. *Peptide Chemistry*; Springer-Verlag: New York, 1988; pp 55−146 and references therein.

(29) Lower catalyst loadings (5−10 mol %) gave a reduced yield of macrocyclic products. This is often observed for RCM macrocyclizations and is believed to be rooted in the apparently accelerated decomposition of the ruthenium methylidene catalyst species at high dilution. See: Ulman, M.; Grubbs, R. H. *Organometallics* **1998**, *17*, 2484−2489.

(30) Each set of olefin isomers proved inseparable on silica gel. The ratio of olefin isomers was estimated by the relative integration of the olefin peaks in the ^1H NMR spectra.

(31) For interpretation of amide N−H IR stretches in apolar organic solvents, see: (a) Gardner, R. R.; Liang, G.-B.; Gellman, S. H. *J. Am. Chem. Soc.* **1995**, *117*, 3280−3281. (b) Liang, G.-B.; Desper, J. M.; Gellman, S. H. *J. Am. Chem. Soc.* **1993**, *115*, 925−938. (c) Gellman, S. H.; Dado, G. P.; Liang, G.-B.; Adams, B. R. *J. Am. Chem. Soc.* **1991**, *113*, 1164−1173. (d) Rao, C. P.; Nagaraj, R.; Rao, C. N. R.; Balaram, P. *Biochemistry* **1980**, *19*, 425−431.

$CHCl_3$,[32] and therefore, CD measurements in TFE can be correlated to the conformations accessed by the peptides during the RCM reaction. Two negative bands at approximately 203−205 ($\pi-\pi^*$) and 218−222 ($n-\pi^*$) nm are observed for all four compounds; these transitions are characteristic of helical conformations in short peptides. The $n-\pi^*$ absorptions are considerably weaker than those for $\pi-\pi^*$, a trend that has been observed experimentally for numerous short 3_{10}-helical peptides.[33] The ratio $R = [\Theta]_{222}/[\Theta]_{208}$ has been determined by Tonolio et al. to be approximately 0.4 for 3_{10}-helical peptides, while $R \approx 1$ for largely α-helical peptides.[34] The average R value for **3**, **4**, **7**, and **8** is 0.3 in TFE, indicative of predominately 3_{10}-helical conformations.

Importantly, these IR and CD data together suggest that the peptide backbones of acyclic dienes **3** and **4** *are preorganized* in a helical conformation for RCM in apolar organic solvents. Furthermore, the IR band intensities and CD ellipticities for macrocycles **7** and **8** do not appear to differ noticeably from their acyclic precursors **3** and **4**, indicating that dramatic conformational changes did not take place upon macrocyclization.[35]

1D ^{1}H NMR Studies of the Acyclic and Cyclic Peptides. We established the presence of specific intramolecular H-bonds in peptides **3**, **4**, **7**, and **8** by analyzing the solvent dependence of the amide NH chemical shifts in $CDCl_3$−$(CD_3)_2SO$ mixtures (Figure 3)[36] and the temperature dependence of these chemical shifts in $(CD_3)_2SO$ (Tables 2 and 3).[37] Relevant ^{1}H NMR parameters for the amide resonances of peptides **3**, **4**, **7**, and **8** dissolved in several solvents are summarized in Tables 2 and 3 (residues are numbered sequentially from N- to C-termini).

Chemical shift assignments in $CDCl_3$ and $(CD_3)_2SO$ were made using standard ^{1}H spin-decoupling techniques. The Val(1) NHs were distinguished on the basis of the well-established tendency of Boc NH groups to resonate at high field in $CDCl_3$.[38] The Aib(4) NHs were the only sharp singlet NH resonances in the ^{1}H NMR spectra and, therefore, could be unambiguously assigned. The Ser, Hse, and Leu NH resonances could be tentatively assigned by comparison to the NMR data for Karle's peptide **2** and other peptides (in $CDCl_3$ and $(CD_3)_2SO$)[39] with structures similar to those described herein.

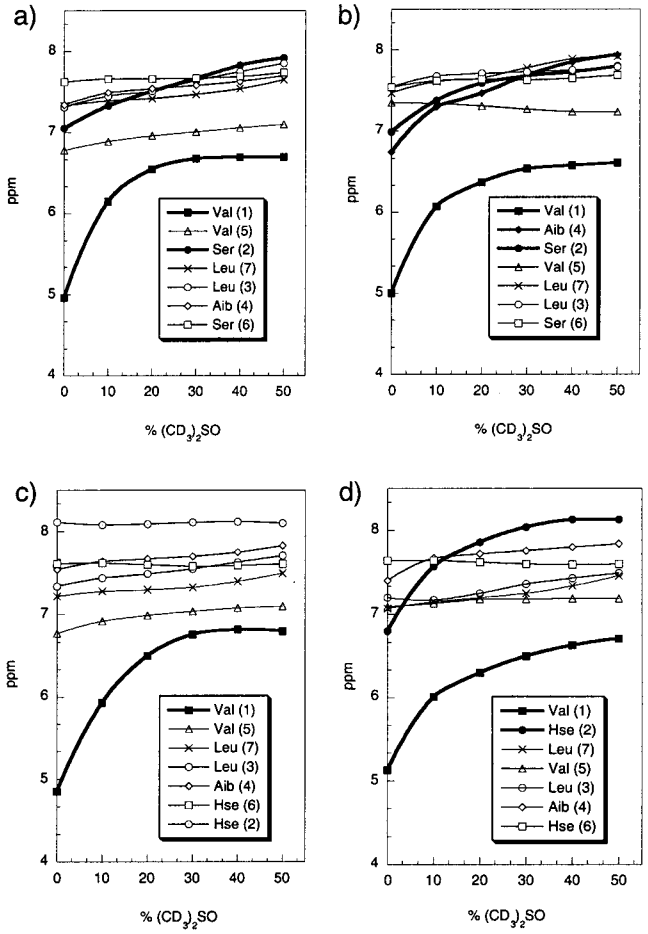

Figure 3. Solvent dependence of NH chemical shifts of (a) acyclic peptide **3**, (b) cyclic peptide **7**, (c) acyclic peptide **4**, and (d) cyclic peptide **8** in $CDCl_3$−$(CD_3)_2SO$ mixtures of varying concentrations. Peptide concentration ~10 mg/mL, 25 °C. Assignments to specific residues are in the legends of each plot. The bold traces correspond to residues believed to be significantly solvent exposed in these solvent mixtures.

We turned to analysis of the $J_{HN\alpha H}$ values in $CDCl_3$ to better establish the identity of these residues. $J_{HN\alpha H}$ values in $CDCl_3$ have been observed to be small at the N-termini of helical peptides (~2−5 Hz) and grow larger toward the C-termini (6−8 Hz).[39] Assuming that the peptides could adopt helical conformations in $CDCl_3$, we cautiously assigned the Ser, Hse, and Leu NHs through analysis of their relative $J_{HN\alpha H}$ values, where coupling constants could be measured (Tables 2 and 3). A similar analysis was not possible in $(CD_3)_2SO$ because the NH $J_{HN\alpha H}$ values were uniformly large; therefore, the relative assignments of Ser, Hse, and Leu in $(CD_3)_2SO$ remain ambiguous.[40] Finally, assignments of the relative spin systems in $CDCl_3$ corroborated well with those made in CD_2Cl_2 using 2D TOCSY[41] and Tr-ROESY[42] techniques (as described below).

Turning to acyclic peptide **3** first, solvent titration experiments (Figure 3a) indicated that only two NH groups, assigned to Val (1) and Ser (2), move appreciably downfield in the NMR spectrum on addition of the

(32) Goodman, M.; Listowsky, I.; Masuda, Y.; Boardman, F. *Biopolymers* **1963**, *1*, 33−42. Details of CD spectral analyses are given in the Experimental Section.

(33) For examples of small helical Aib containing peptides exhibiting similar CD ellipticities in TFE, see: (a) Banerjee, A.; Raghothama, S.; Balaram, P. *J. Chem. Soc., Perkin Trans. 2* **1997**, 2087−2094. (b) Karle, I. L.; Banerjee, A.; Bhattachrjya, S.; Balaram, P. *Biopolymers* **1996**, *38*, 515−526.

(34) Toniolo, C.; Polese, A.; Formaggio, F.; Crisma, M.; Kamphuis, J. *J. Am. Chem. Soc.* **1996**, *118*, 2744−2745.

(35) From these data alone we cannot rule out the possibility of a conformational switch from an α- to a 3_{10}-helix (or vice versa) upon ring-closure. See: Yoder, G.; Polese, A.; Silva, R. A. G. D.; Formaggio, F.; Crisma, M.; Broxterman, Q. B.; Kamphuis, J.; Toniolo, C.; Keiderling, T. A. *J. Am. Chem. Soc.* **1997**, *119*, 10278−10285.

(36) (a) Pitner, T. P.; Urry, D. W. *J. Am. Chem. Soc.* **1972**, *94*, 1399−1400.

(37) (a) Hruby, V. J. *Chemistry and Biochemistry of Amino Acids, Peptides and Proteins*; Weinstein, B., Ed.; Dekker: New York, 1974; Vol. 3, pp 1−188. (b) Kopple, K. D.; Ohnishi, M.; Go, A. *J. Am. Chem. Soc.* **1969**, *91*, 42646-4272. (c) Ohnishi, M.; Urry, D. W. *Biochem. Biophys. Res. Commun.* **1969**, *36*, 194−202.

(38) (a) Bystrov, V. F.; Portnova, S. L.; Tsetlin, V. I.; Ivanov, V. T.; Ovchinnikov, Y. A. *Tetrahedron* **1969**, *25*, 493−515. (b) Nagaraj, R.; Balaram, P. *Biochemistry* **1981**, *20*, 2828−2835.

(39) Iqbal, M.; Balaram, P. *J. Am. Chem. Soc.* **1981**, *103*, 5548−5552.

(40) Assignment of the relative spin systems in $(CD_3)_2SO$ by 2D NMR techniques is currently underway in our laboratory.

(41) Braunschweiler, L.; Ernst, R. R. *J. Magn. Reson.* **1983**, *53*, 521−528.

(42) Bax, A.; Davis, D. G. *J. Magn. Reson.* **1985**, *65*, 355−360.

Table 2. NMR Parameters of Amide NH Groups in Peptides 3 and 7

		$CDCl_3$		$(CD_3)_2SO$[b]		
peptide	residues[a]	δ_{NH} (ppm)	$^3J_{HNC^aH}$ (Hz)	δ_{NH} (ppm)	$^3J_{HNC^aH}$ (Hz)	$d\delta/dT$[c] (ppb/K)
3	Val (1)	4.96	–[d]	6.81	8.5	6.9
	Ser (2)	7.05	5.0	7.96	–[e]	5.3
	Leu (3)	7.31	6.1	8.05	7.3	5.3
	Aib (4)	7.34	–	7.93	–	5.5
	Val (5)	6.78	6.3	7.09	7.8	1.7[f]
	Ser (6)	7.62	8.0	7.96	–[e]	4.3
	Leu (7)	7.33	8.6	8.10	7.7	6.7
7	Val (1)	5.00	–[d]	6.78	8.7	6.0
	Ser (2)	6.99	–[d]	7.92	–[e]	4.9
	Leu (3)	7.47	6.6	7.95	7.8	3.0
	Aib (4)	6.74	–	8.02	–	3.9
	Val (5)	7.35	8.9	7.33	7.6	2.2[f]
	Ser (6)	7.54	–[e]	7.90	–[e]	5.1
	Leu (7)	7.54	–[e]	8.10	7.7	5.9

[a] Val, Ser, and Leu NHs were assigned using spin decoupling. Relative assignment of the Val, Ser, and Leu NHs is not unequivocal (see text). [b] Spectra were measured at 298 K and at a 10 mg/mL sample concentration. [c] $d\delta/dT$ is the temperature coefficient of the NH chemical shifts. [d] Peak not resolved; apparent singlet. [e] Peak not resolved due to overlap. [f] This $d\delta/dT$ value is indicative of a solvent-shielded NH.

strongly H-bonding solvent, $(CD_3)_2SO$, to solutions of the apolar solvent, $CDCl_3$. Clearly, in solutions of up to 50% $(CD_3)_2SO$, the remaining five NH groups are shielded from solvent, strongly supporting a completely helical conformation in which the NH groups of residues 3–7 are intramolecularly H-bonded. A completely 3_{10}-helical sequence with five 4 → 1 H-bonds is consistent with these data. However, structures involving both 4 → 1 and 5 → 1 H-bonding patterns with the Boc C═O accepting H-bonds from both the Leu(3) and the Aib(4) NH groups cannot be ruled out.[43]

The analogous solvent titration experiment conducted on solutions of cyclic peptide **7** also established that its corresponding Val(1) and Ser(2) NH groups are significantly solvent exposed (Figure 3b), potentially indicative of a similar 3_{10}-helical conformation. Interestingly, however, the Aib(4) NH in peptide **7** also appears to be solvent exposed. This suggests that the helical conformation of **3** is slightly disrupted upon cyclization to give **7**, with the Aib(4) in peptide **7** no longer able to form the 4 → 1 H-bond present in **3**. Notably, the Aib(4) residue is in the center of the macrocyclic substructure of **7** and could potentially be conformationally disturbed by the cyclization.

Temperature-gradient NMR experiments in $(CD_3)_2SO$ of **3** and **7** yielded very similar conformational data for both peptides (Table 2). The majority of the temperature coefficients ($-d\delta/dT$) of the NH groups in both **3** and **7** are high (≥4 ppb/K), with the exception of those for the Val (5) NHs, which have values of 1.7 and 2.2 ppb/K, respectively (highlighted in Table 2). This is suggestive of a completely nonhelical conformation in $(CD_3)_2SO$, with an isolated weak Leu(3)-Aib(4) β-turn, stabilized by a 4 → 1 H-bond between the Ser(2) C═O and the Val(5) NH groups. Such X-Aib β-turns are common features in small Aib-containing peptides.[23] Interestingly, the Leu(3) NH of cyclic peptide **7** has a moderately low $d\delta/dT$ value of 3.0 ppb/K, which suggests that the Leu(3) NH of **7** is also involved in weak H-bonding in $(CD_3)_2SO$. We speculate that the Leu(3) NH could be involved in a weak 4 → 1 β-turn-type H-bond with the Boc C═O. Finally, the $J_{HNC\alpha H}$ values for all the NH groups in peptides **3** and **7** are uniformly high (≥8 Hz) in $(CD_3)_2SO$ (Table 2), which is characteristic of extended peptide conformations.[44] These data, taken together with the $d\delta/dT$ values and the solvent titration data above, are supportive of predominantly 3_{10}-helical conformations for both **3** and **7** in $CDCl_3$, which are almost completely disrupted in the more strongly solvating medium, $(CD_3)_2SO$.

Turning next to the NMR experiments conducted on acyclic homologue **4** and macrocycle **8**, we observed behavior in $CDCl_3$ and $(CD_3)_2SO$ solutions that was somewhat similar to peptides **3** and **7** (Table 3, Figure 3c,d). In the solvent titration experiment for acyclic peptide **4**, only the Val(1) NH moved markedly downfield upon the addition of the more polar solvent $(CD_3)_2SO$ (Figure 3c). The remaining six amide NH groups of **4** show very small changes in chemical shift in up to 1:1 mixtures of the $(CD_3)_2SO$ and $CDCl_3$, again characteristic of intramolecularly H-bonded NH groups. This suggests that the five intramolecular 4 → 1 H-bonds present in acyclic peptide **3** are also maintained in its bis-Hse homologue **4**, plus an additional H-bond at the N-terminus involving the Hse(2) NH. We tentatively assigned Hse(2) NH to be involved in an H-bond with either the Hse(2) δ oxygen or the Boc carbonyl oxygen **4**; this was later established by 2D NMR/molecular modeling analyses (as described below).

The analogous solvent titration experiments were conducted on cyclic peptide **8** (Figure 3d), and the extra Hse(2) H-bond observed in peptide **4** was not observed. Instead, in analogy to peptide **3** (Figure 3a), only the Val(1) and Hse(2) NHs moved downfield upon addition of $(CD_3)_2SO$, while the other five amide NHs remained constant. Therefore, cyclic peptide **8** was assumed to have a 3_{10}-helical conformation similar to that of acyclic peptide **3** in solutions containing up to 50% $(CD_3)_2SO$, with five intramolecular amide H-bonds. Interestingly, cyclic peptide **8** lost one H-bond relative to its acyclic precursor **4**, suggesting that **8**, like related cyclic peptide **7**, undergoes a subtle conformational shift upon cyclization. Again, as in the analysis of peptide **3** and **7**, we could not rule out the possibility of 4 → 1 and/or 5 → 1 H-bonding patterns at the N-termini of peptides **4** and **8** from these experiments alone.

The temperature-gradient NMR experiment conducted on acyclic peptide **4** suggests it assumes an extended conformation in $(CD_3)_2SO$ similar to peptides **3** and **7**. All of the observed $-d\delta/dT$ values for the NH groups were high (≥4 ppb/K) except for Val(5), which had a $-d\delta/dT$ value of 2.8 ppb/K (highlighted in Table 3). In analogy to peptides **3** and **7** above, this was believed to be indicative of a weak 4 → 1 H-bond between the Hse(2) C═O and the Val(5) NH group in the context of a Leu(3)-Aib(4) β-turn. This, along with the fairly high $J_{HNC\alpha H}$ values for **4** in $(CD_3)_2SO$ (Table 3), suggests that peptide **4** assumes a very loosely structured conformation in $(CD_3)_2SO$. Finally, the $-d\delta/dT$ values for cyclic peptide **8** in $(CD_3)_2SO$ follow the same pattern as peptide **7**, with the Val(5) NH and Leu(3) having moderately low $-d\delta/$

(43) Such H-bonding patterns with a mixed 3_{10}/α-helical turn are often found at the N-termini of α-helical peptides. See ref 26.

(44) (a) Wüthrich, K. *NMR of Proteins and Nucleic Acids*, Wiley-Interscience: New York, 1986. (b) Wüthrich, K.; Billeter, M.; Braun, W. *J. Mol. Biol.* **1984**, *180*, 715–740.

Table 3. NMR Parameters of Amide NH Groups in Peptides 4 and 8

		$CDCl_3$		CD_2Cl_2		$(CD_3)_2SO$[b]		
peptide	residues[a]	δ_{NH} (ppm)	$^3J_{HNC\alpha H}$ (Hz)	δ_{NH} (ppm)	$^3J_{HNC\alpha H}$ (Hz)	δ_{NH} (ppm)	$^3J_{HNC\alpha H}$ (Hz)	$d\delta/dT$[c] (ppb/K)
4	Val (1)	4.85	2.4	5.03	2.0	6.81	8.2	6.9
	Hse (2)	8.11	3.4	8.11	3.4	7.82	7.8	4.0
	Leu (3)	7.34	5.7	7.37	6.4	7.91	—[d]	4.7
	Aib (4)	7.54	—	7.61	—	8.08	—	6.1
	Val (5)	6.77	6.8	6.89	6.4	7.12	7.3	2.8[e]
	Hse (6)	7.61	8.3	7.55	8.1	7.96	7.3	3.6
	Leu (7)	7.22	8.3	7.21	8.1	7.93	—[d]	5.3
8	Val (1)	5.13	—[f]	5.17	2.0	6.84	8.9	6.4
	Hse (2)	6.80	—[f]	6.76	3.9	7.99	7.4	3.3
	Leu (3)	7.20	3.0	7.24	3.9	7.71	6.1	3.9
	Aib (4)	7.40	—	7.48	—	8.00	—	3.5
	Val (5)	7.09	—[d]	7.83	7.8	7.28	7.9	2.9[e]
	Hse (6)	7.64	8.4	7.55	8.8	7.84	7.4	4.4
	Leu (7)	7.07	—[d]	7.05	8.3	8.03	7.9	6.3

[a] Val, Hse, and Leu NHs were assigned using spin decoupling. Relative assignment of the Val, Hse, and Leu NHs is not unequivocal (see text). [b] Spectra were measured at 298 K and at a 10 mg/mL sample concentration. [c] $d\delta/dT$ is the temperature coefficient of the NH chemical shifts. [d] Peak not resolved due to overlap. [e] This $d\delta/dT$ value is indicative of a solvent-shielded NH. [f] Peak not resolved-apparent singlet.

dT values of 2.9 and 3.3 ppb/K, respectively. Coupling this trend with the large $J_{HNC\alpha H}$ values for **8** in $(CD_3)_2SO$, we tentatively assigned cyclic peptide **8** to have a fairly unstructured conformation in $(CD_3)_2SO$. However, qualitatively, the lower $-d\delta/dT$ value for the Leu(3) NH in both macrocycles **7** and **8** suggest that the C−C tether is constraining the peptides to a slightly more rigid conformation in $(CD_3)_2SO$ than their acyclic precursors.

The ^1H NMR experiments above indicate that peptides **3**, **4**, **7**, and **8** adopt predominantly 3_{10}-helical structures in $CDCl_3$ and that these helical structures are disrupted in the more solvating medium, $(CD_3)_2SO$. The latter trend dispelled our initial hopes that the covalent link installed in macrocycles **7** and **8** would force them to maintain rigid, helical conformations, even in strongly H-bonding media. Importantly, however, these data suggested that acyclic peptides **3** and **4** were preorganized in a helical conformation in $CDCl_3$ for RCM macrocyclization, and that this conformation was maintained in the cyclic products **7** and **8**. Interestingly, the data obtained for Karle's peptide **2** in the analogous NMR experiments were almost identical,[25] suggesting that replacement of the two Ala resides in **2** (residues believed to be strongly helix-promoting)[45] with Ser or Hse (*O*)-allyl ethers did not act to disrupt the 3_{10}-helical predisposition of the peptide backbones.

X-ray Crystal Structure of Cyclic Peptide 8. Both cyclic peptides **7** and **8** exhibited higher crystallinity than their acyclic precursors **3** and **4**, respectively. Slow evaporation of **8** from CH_2Cl_2/hexane provided crystals suitable for X-ray crystallographic analysis (Figure 4).[46]

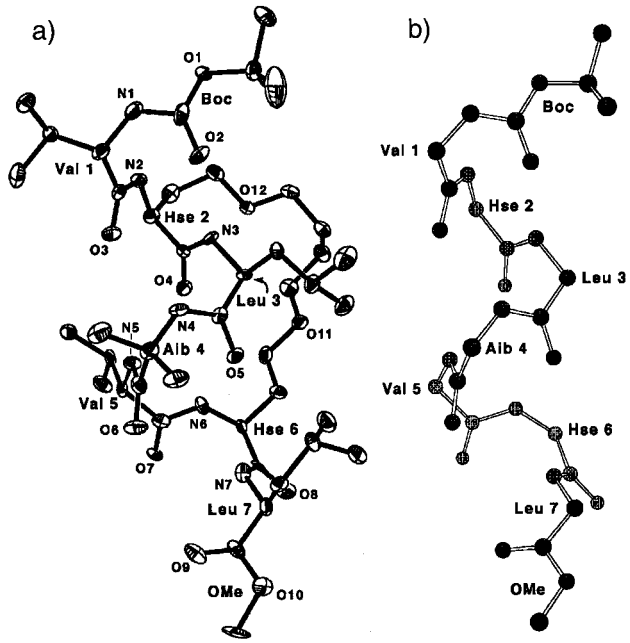

Figure 4. (a) ORTEP diagram of X-ray crystal structure of cyclic peptide **8**. Thermal ellipsoids represent 30% probability levels. Hydrogen atoms have been omitted for clarity. (b) Rendering of **8** without amino acid side chains.

Pertinent torsion angles from the structure of **8** are listed in Table 4.[47] Viewing the peptide from the N- to C-terminus, it appears that the peptide backbone is helical for the first five residues and then has characteristic fraying over the final two.[48] The average torsional angles ϕ (about N−C$^\alpha$) and ψ (about C$^\alpha$−C′) for the first five residues are −57° and −34°, respectively, which approximate those for a right-handed 3_{10}-helix (−57° and −30°).[49] These torsional angles are marginally close to

(45) O'Neil, K. T.; DeGrado, W. F. *Science* **1990**, *250*, 646−651.

(46) Colorless crystals of **8** were grown from CH_2Cl_2/hexane: crystal size 0.3 × 0.5 × 0.5 mm, orthorhombic, space group $P2_12_12_1$, $Z = 4$, $a = 19.30(1)$ Å, $b = 24.73(2)$ Å, $c = 12.134(7)$ Å, $V = 5791(6)$ Å^3, $\rho_{calcd} = 1.246$ g cm^{-3}; $2\theta = 1.6-50.0°$ (Mo Kα, $\lambda = 0.7107$ Å, graphite monochromator, $2\theta - \theta$ scan, $T = 156$ K); 4698 reflections measured, 2266 unique data used [$I > 3.0\sigma(I)$]; no absorption corrections were applied; direct methods (SHELXTL 86), refinement with full-matrix least-squares methods, hydrogen atoms refined isotropically, all other atoms refined anisotropically; $R = 0.066$, $R_W = 0.077$; maximum residual electron density 0.80 e/Å^3; GOF = 2.28 for 633 variables. Crystallographic data (excluding structure factors) for structure **8** have been deposited with the Cambridge Crystallographic Data Centre as supplementary publication no. CCDC-101810. A full copy of the crystallographic data for structure **8** (excluding structure factors) can be found in the Supporting Information.

(47) For standard definitions of the torsion angles for rotations about bonds of peptide backbones (ϕ, ψ, and ω) and amino acid side chains (χ^n), see: IUPAC−IUB Commission on Biochemical Nomenclature. *Biochemistry* **1970**, *9*, 3471−3479.

(48) Residues at the ends of peptide helices are often irregular in conformation. This effect is more pronounced at the C-terminus. See: Chothia, C. *Annu. Rev. Biochem.* **1984**, *53*, 537−572.

(49) Toniolo, C.; Benedetti, E. *Trends Biochem. Sci.* **1991**, *16*, 350−353.

Table 4. Torsional Angles for 8 (Deg)

residue	ϕ	ψ	ω	χ^1	χ^2
Val (1)	−52[a]	−40	−174	167, −71	
Hse (2)	−53	−28	−178	71	
Leu (3)	−60	−37	−180	176	−178, 61
Aib (4)	−55	−36	−178		
Val (5)	−65	−30	−170	176, −62	
Hse (6)	−85	−15	−167	−62	
Leu (7)	−109	165[b]	−180[c]	−61	−178, −55

[a] C′ (0), N (1), Cα (1),C′ (1). [b] N (7), Cα (7), C′ (7), O (OMe). [c] Cα (7), C′ (7), O (OMe), C (OMe).

Table 5. Hydrogen Bonds for 8

type	donor[a]	acceptor	N···O (Å)	angle (deg) C═O···N
interpeptide	N(1)[b]	O(5′)[c]	2.930	158
4 → 1	N(3)	O(0)[d]	3.014	131
4 → 1	N(4)	O(1)	2.993	130
4 → 1	N(5)	O(2)	2.970	117
4 → 1	N(6)	O(3)	2.957	118

[a] Carbonyl oxygens O(4), O(6), and O(7) and amide nitrogens N(2) and N(7) do not appear to be involved in any H-bonding. [b] Numbers correlate with residue number from N- to C-terminus. [c] Val(5) carbonyl of the adjacent peptide in the unit cell. [d] Corresponds to Boc group carbonyl.

those for the average right-handed α-helix ($\phi = -63°$, $\psi = -42°$), and therefore, from these data alone, it is difficult to completely exclude the possibility of peptide **8** being α-helical or accessing a mixed α/3_{10}-helix conformation in the solid-state.

Analysis of the amide N to carbonyl O distances (N···O) and respective angles (N···O═C), however, supports the presence of four consecutive 4 → 1 intramolecular H-bonds (2.96−3.01 Å), involving N(3)−N(6) and O(2)−O(5), which are diagnostic of a 3_{10}-helix (Table 5).[50] This iterative H-bonding pattern involves the carbonyl O and amide NH of amino acids that are separated by two residues.[51] We speculate that the Leu(3) carbonyl O(5) could also be involved in a fifth extremely long 5 → 1 H-bond with the Leu(7) amide N(7) (N···O 3.50 Å), which may be lengthened due to the disorder of the helix at the C-terminus. Thereafter, the 4 → 1 H-bonding pattern is continued intermolecularly in a head-to-tail fashion, with the Val(5) carbonyl O(7) H-bonding to the Val(1) Boc amide N(1) (N···O 2.91 Å) of the adjacent peptide molecule in the unit cell. In fact, all the peptide helix axes are parallel in the unit cell of **8**; such infinite head-to-tail H-bonding is commonly observed in crystalline hydrophobic peptide helices.[23,52] The evidence suggests that replacement of the two Ala residues in peptide **2** with tethered Hse residues in peptide **8** has induced the peptide backbone to transform from an α-helix to a predominantly 3_{10}-helix in the solid state. The constraint imposed by the side-chain linkage in peptide **8** could be cause for this conformational shift.[53]

Two views comparing the X-ray structures of Karle's peptide **2** and cyclic heptapeptide **8** are shown in Figure 5. Viewing the two helical structures side-on (Figure 5a,b), it is apparent qualitatively that cyclic peptide **8** is longer from N- to C-termini than peptide **2**, which corroborates with the longer average length of 3_{10}-helices versus α-helices due to the shorter helical pitch in 3_{10}-helices (3.0 residues versus 3.6 residues per turn of the helix, respectively).[48] This difference in pitch is also apparent in Figure 5c,d, where two views along the helix axes of peptides **2** and **8** are shown (from the N- to C-termini). Both structure views show a pseudocircular arrangement of amide NH groups about the axis of the helix, an arrangement frequently observed in helical peptide and protein structures.[23] However, the circumference of the circular core in cyclic peptide **8** is considerably smaller than that of α-helical peptide **2**, which is further qualitative evidence of peptide **8** adopting a more tightly wound, 3_{10}-helical conformation.

Solution-Phase NMR Structures of Acyclic Peptide 4 and Cyclic Peptide 8. With a crystal structure in hand, we next investigated the solution-phase structure of acyclic peptide precursor **4** and cyclic peptide **8** in CD_2Cl_2 employing 2D ^{1}H NMR techniques and molecular modeling. It is common for short peptides (less than 10 residues) to adopt numerous, rapidly interconverting low-energy conformations in solution.[54] NMR spectra of such systems often show only a time-averaged behavior and it is misleading to attempt to fit the NMR data to a single structure. However, as observed with Karle's peptide **2**, we believed that the Aib residues in heptapeptides **4** and **8** would act to stabilize a more rigid structure in solution, which could lend itself to a structure elucidation using NMR and molecular modeling.[55] Additionally, we hypothesized that cyclic peptide **8** would adopt a more rigid conformation than its acyclic precursor **4** due to the presence of the intramolecular C−C bond tether.

All NMR measurements were made at room temperature on a Bruker DPX 400 MHz spectrometer, and data was processed using XWINNMR 2.6. NMR samples were prepared by dissolving peptides **4** and **8** in CD_2Cl_2 (c = 30 mM), after which time the samples were degassed and sealed under Argon. CD_2Cl_2 was selected for use as solvent because it offered the best dispersion of NH and $C^{\alpha}H$ chemical shifts (Table 3).[56,57] Representative plots of the ^{1}H NMR spectra of peptides **4** and **8** in CD_2Cl_2 are shown in Figure 6. 1D ^{1}H, 2D TOCSY,[41] 2D Tr-ROESY,[42] and 1D GOESY[58] experiments were used for proton chemical shift assignments and Overhauser effect measurements. For both the TOCSY and Tr-ROESY spectra,

(50) The 4 → 1 N···O═C angles for these four H-bonds range from 118 to 131°.

(51) The analogous H-bonding pattern in α-helices is 5 → 1, spanning three residues. See ref 48.

(52) Views of the unit cell of cyclic peptide **8** can be found in the Supporting Information.

(53) The different medium from which **2** and **8** were crystallized (CH_2Cl_2/hexane for **8**; methanol/H_2O for **2**) may contribute to the disparity in their crystal structures.

(54) Kessler, H.; Bermel, W. Conformational Analysis of Peptides by Two-Dimensional NMR Spectroscopy. In *Applications of NMR Spectroscopy to Problems in Stereochemistry and Conformational Analysis*; Takeuchi, Y., Marchand, A. P., Eds.; Methods in Stereochemical Analysis Series; VCH Publishers: Deerfield Beach, FL, 1986; Vol. 6, pp 179−205.

(55) Gratias et al. have recently disclosed work towards defining a peptide model for the 3_{10}-helical conformation in solution. For their 2D NMR structural analysis of a 3_{10}-helical heptapeptide in $CDCl_3$, coupled with X-ray diffraction; see: Gratias, R.; Konat, R.; Kessler, H.; Crisma, M.; Valle, G.; Polese, A.; Formaggio, F.; Toniolo, C.; Broxterman, Q. B.; Kamphuis, J. *J. Am. Chem. Soc.* **1998**, *120*, 4763−4770.

(56) NMR assignments of the relative spin systems of **4** and **8** in CD_2Cl_2 corroborated very well with those made in $CDCl_3$, which we deemed indicative of peptide **4** and **8** adopting similar conformations in both solvents. Furthermore, RCM of **3** and **4** in CH_2Cl_2 gave yields of macrocyclic products **5** and **6** similar to those in $CDCl_3$.

(57) Full NMR assignments for peptides **4** and **8** in CD_2Cl_2, tables of interproton distance restraints, Ramachandran maps and SYBYL mol2 files of the calculated structures can be found in the Supporting Information.

(58) Stott, K.; Stonehouse, J.; Keeler, J.; Hwang, T. L.; Shaka, A. J. *J. Am. Chem. Soc.* **1995**, *117*, 4199−4200.

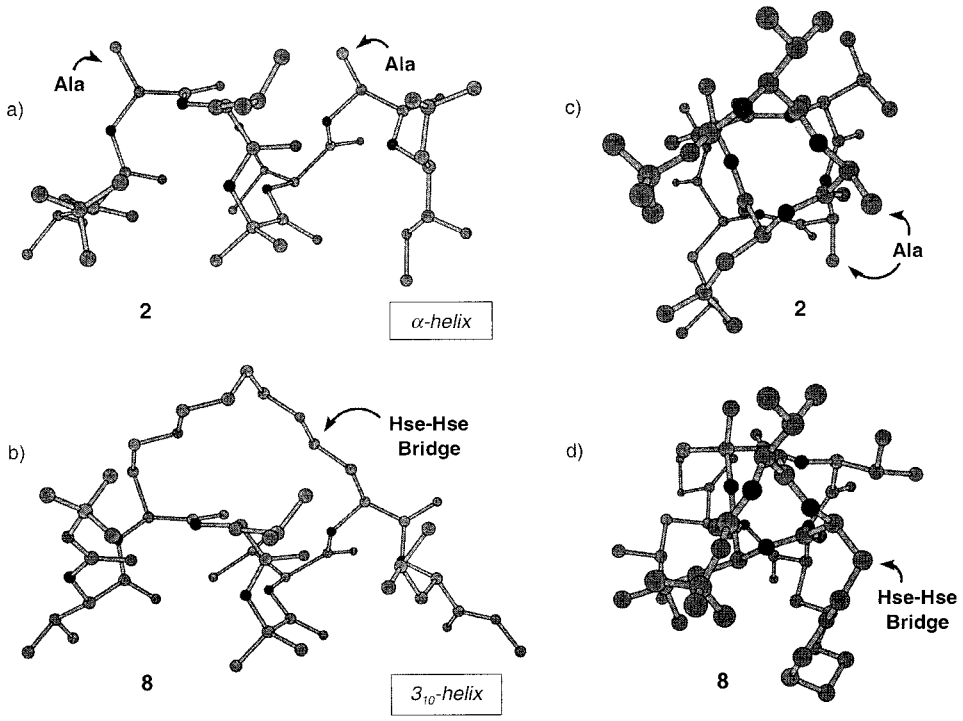

Figure 5. Chem3D views of the solid-state structures of Karle's peptide **2** and cyclic peptide **8** from N- to C-termini (from left to right (a, b) and along the helix axis (c, d)). The two Ala side chains of **2** and the Hse-Hse C−C bridge of **8** are designated with arrows.

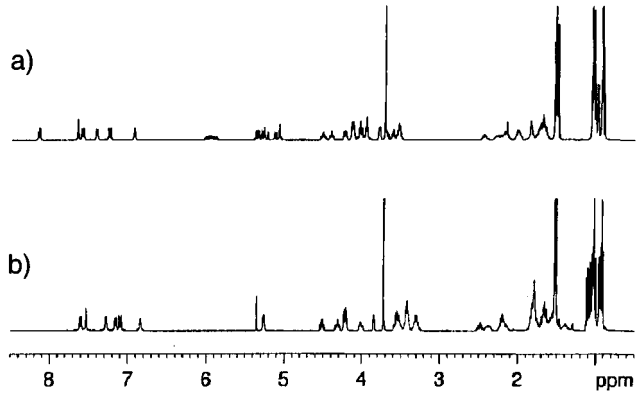

Figure 6. Plots of the 400 MHz ^{1}H NMR spectra of (a) acyclic peptide **4** and (b) hydrogenated cyclic peptide **8**. Peptide concentration ~10 mg/mL in CD_2Cl_2, 25 °C.

a 2048 × 256 data matrix was collected with 16 scans/FID. The Tr-ROESY spectrum was acquired with a 600 ms composite spin-lock pulse. GOESY spectra were acquired with a 250 ms mixing time, 512 scans, and 16K data points.[59] The cross-peaks in the Tr-ROESY spectra were integrated to calculate interproton distance restraints.[60] Representative portions of the Tr-ROESY spectra are shown in Figure 7. Using rules established by Wüthrich,[44] conservative interproton distance restraints (i.e., upper bounds only) were calculated based upon the integrated intensity of Tr-ROESY cross-peaks and through-bond relationships between the protons giving rise to the cross-peak.[61]

Two rounds of restrained conformational searching were conducted for both heptapeptides **4** and **8** using the RandomSearch algorithm of SYBYL 6.6 (Tripos Software, St. Louis, MO).[62] We assumed the conformations of peptides **4** and **8** in solution would be similar to those in the solid state, and thus, the crystal structure of peptide **8** (see above) was used as the starting structure for the RandomSearches of both acyclic peptide **4** (with concurrent removal of the covalent tether using SYBYL) and cyclic peptide **8**.[63] Initial conformational searches employed distance restraints that were calculated from unambiguously assigned Tr-ROESY cross-peaks. Conformers found with energies 5 kcal/mol higher than that of the lowest energy conformer (representing less than 1% of all solution conformers in a Boltzmann distribution) were discarded. If all low-energy conformers allowed elucidation of a previously ambiguously assigned ROE cross-peak, and if GOESY data indicated presence of an Overhauser effect, the corresponding restraint was added to the original set for the refinement round of calculation.

(59) The 1D GOESY experiment was preferable to a standard 1D NOE difference experiment because it was designed to reduce incomplete subtraction artifacts. Furthermore, because GOESY is a 1D experiment, it offered better resolution and higher S/N ratios than the 2D Tr-ROESY. GOESY spectra were thus used to confirm or refute weak or ambiguous ROEs.

(60) While the more standard practice is to integrate NOESY cross-peaks to obtain distance information, the conservative manner in which the integrals were used and the fact that ROEs do not pass through a null (commonly observed for NOEs in peptides of this size), resulted in the use of ROESY data.

(61) A correction factor of 1 Å was added for methyl groups and proton pairs that could not be stereospecifically assigned.

(62) The RandomSearch algorithm for each run searched conformational space in two steps, repeated in sequence for 2000 total iterations: (step 1) random rotation of up to 3 torsional angles in the molecule, and (step 2) restrained energy minimization of the resulting structure using the static Merck Molecular Force-Field, MMFF94s. See: Halgren, T. *J. Comput. Chem.* **1999**, *20*, 720−729.

(63) As the RandomSearches of these peptides were not initiated from a number of different starting structures, we cannot conclude that the results were independent of initial conditions. However, the preponderance of solution-phase data in support of the conformations found (including the IR, CD, $CDCl_3$−$(CD_3)_2SO$ titration data and the set of observed ROEs), permits the conclusions reported here to be made.

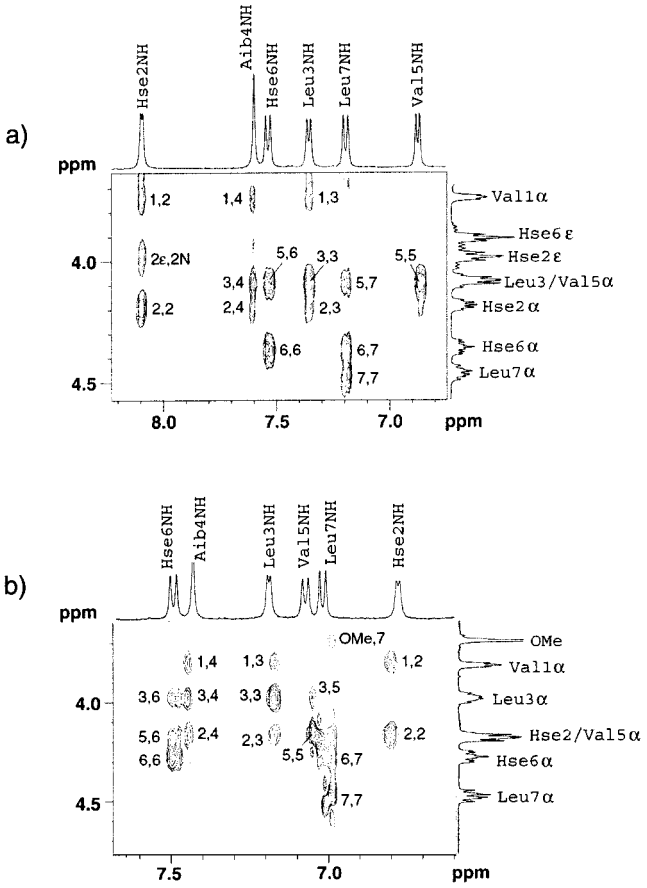

Figure 7. Partial Tr-ROESY spectra for (a) acyclic peptide **4** and (b) cyclic peptide **8** in CD_2Cl_2 (30 mM) at 25 °C showing $C^{\alpha}H-NH(i+1)$ ROEs. (2048 × 256 data matrix, 16 scans/FID, 600 ms composite spin-lock pulse.)

Refined conformations of **4** and **8** were calculated using a total of 32 and 35 distance restraints, respectively.[57] All refined structures with calculated energies within 5 kcal/mol of that of the lowest energy refined structure were considered reasonable solution conformers.

The majority of the Tr-ROESY cross-peaks employed to calculate the restraints were prototypical of α- or mixed α/3_{10}-helical conformations (Figure 8). For example, the observed NH−NH(i,i + 1) ROEs are characteristic of α- and 3_{10}-helices, but can also be found in Type 1 β-turns.[44] The longer range $C^{\alpha}H$-NH(i,i + 2) and $C^{\alpha}H$-NH(i,i + 3) ROEs, added as restraints in the second round of calculation, are more diagnostic of 3_{10}- and mixed α/3_{10}-helical conformations, respectively. However, additional cross-peaks, including three $C^{\alpha}H$-NH(i,i + 1) connectivities, suggested that the acyclic peptide (**4**) may not be perfectly helical.

The refined conformer families of acyclic peptide **4** calculated from the RandomSearch procedure are overlaid in Figure 9a. Five main conformer families were generated (average backbone-RMSD across all families: 0.9 ± 0.94 Å) that differed from each other primarily in their respective Leu (7) $\phi-\psi$ angles. Minimized energies were in the range 44−48 kcal/mol, with no distance restraint violation energies rising above 0.3 kcal/mol. The conformers found had partial 3_{10}-helical character at the Hse (2), Aib (4), and Val (5) residues, but many conformers also had considerable deviation from helicity at Val (1), Leu (3), and at their C-termini. Interestingly, in all conformers found, the Hse (2) NH proton was H-bonded

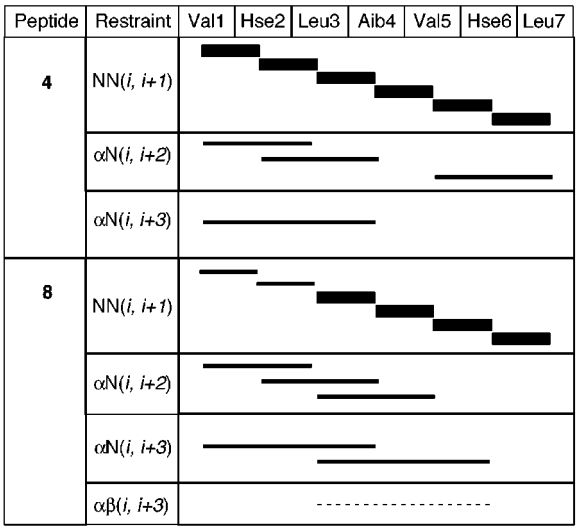

Figure 8. Summary of sequential and medium range ROE data for acyclic peptide **4** and cyclic peptide **8**. ROE intensities are classified as strong (upper distance constraint 3.0 Å, thick line), medium (4.0 Å, thin line), and weak (5.0 Å, dotted line).

to either the Hse (2) δ oxygen or the Boc carbonyl oxygen. This could possibly explain the NMR solvent titration experiments for **4** (Figure 3c), which suggested that the Hse (2) NH proton was involved in H-bonding in predominately $CDCl_3$ solutions (see above).

The set of ROESY cross-peaks utilized to calculate restraints for cyclic peptide **8** were more definitive of a helical structure than those of its acyclic precursor (**4**) (Figure 8). Specifically, the three $C^{\alpha}H$-NH(i,i + 2) cross-peaks found are generally observed only for 3_{10}-helices, whereas the six NH-NH(i,i + 1), two $C^{\alpha}H$-NH(i,i + 3), and one $C^{\alpha}H$-$C^{\beta}H$(i,i + 3) cross-peaks found are typical of either α- or 3_{10}-helices.[44] However, in analogy to acyclic peptide **4**, some $C^{\alpha}H$-NH(i,i + 2) connectivities could be found in the ROESY spectrum of **8**, which indicated some conformational deviation from helicity.

The overlaid conformers of cyclic peptide **8** calculated in the RandomSearches expose only a single conformer family (Figure 9b), with a backbone-RMSD of 0.04 ± 0.044 Å. The conformer family had an average energy of 39.2 kcal/mol, and an average distance restraint violation energy of 0.1 kcal/mol, which indicated good agreement with NMR data. The refined conformation of cyclic peptide **8** was characterized primarily as a well-defined 3_{10} helix up to the fifth residue, with four consecutive 4 → 1 H-bonds. This corroborated very well with the solid-state structure of **8** (Figure 4, Table 5). Consistent with the solvent titration experiments conducted on cyclic peptide **8** (Figure 3d), the Hse (2) NH proton was not involved in H-bonding in any of the structures found. Interestingly, the Leu (7) NH was not involved in H-bonding either, which is inconsistent with the solvent titration studies. This amide proton did, however, point inward toward the helical axis in the refined solution structures, which suggests it is sequestered from solvation.

All of the conformers found for acyclic peptide **4** had more deviations from helicity in the $\phi-\psi$ values[57] and in the H-bonding pattern than those for cyclic peptide **8**. Additionally, the fact that such a multitude of conformers were found for the acyclic peptide (**4**) indicates that, without the covalent tether, convergence of the molecule

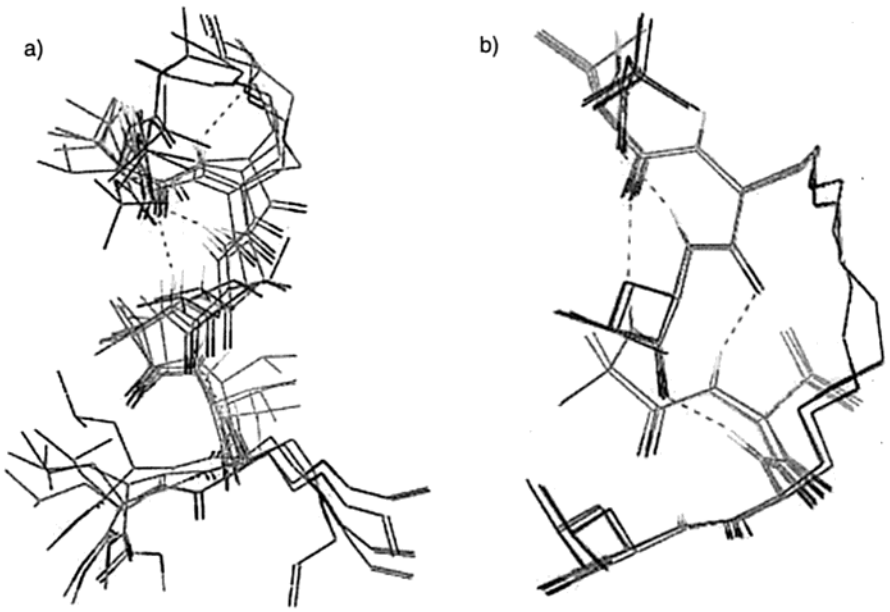

Figure 9. Overlaid low energy conformers from the structure families generated for (a) acyclic peptide **4** and (b) cyclic peptide **8**. Dotted gray lines represent H-bonds.

to a single conformation could not be achieved. These data suggest that the covalent tether in cyclic peptide **8** better stabilized a 3_{10}-helical conformation in solution than just the Aib residue alone.

Finally, it is interesting that the intramolecular C−C tether in the refined conformers for cyclic peptide **8** was not parallel to the helical axis (Figure 9b). If the conformers found were α- instead of 3_{10}-helical, the tether would have been parallel to the helical axis, since the attachment points at the (*i*) and (*i* + 4) positions are directly above each other in a perfect α-helix. Instead, the more elongated, tighter 3_{10}-helical conformation of the peptide backbone causes an extrusion of the tether. As discussed earlier, NMR data for peptides **3** and **7** with *O*-allyl Ser at the (*i*) and (*i* + 4) positions also indicate that they both adopt predominantly 3_{10}-helical conformations in apolar solvents. Notably, the C−C tether in the bis-Ser peptide macrocycle **7** is two methylene groups shorter than that of cyclic peptide **8**. The Aib (4) NH in **7** was significantly solvated in its calculated solution structure (data not shown), which was also observed in the NMR solvent titration studies (Figure 3b), indicating a loss of the Aib (4) NH → Val (1) C═O H-bond upon cyclization. This suggests that the shorter C−C tether in **7** was simply not long enough to allow for a perfect 3_{10}-helix, and it caused a central "kink" in the peptide backbone at the Aib residue. Future work will study the placement of *O*-allyl Ser residues at the (*i*) and (*i* + 3) positions, instead of the (*i*) and (*i* + 4), as this could be a better design strategy for the covalent capture of certain 3_{10}-helical peptide macrocycles.[64]

Summary and Future Outlook

Helical peptide dienes have been treated with alkylidene **1** to afford macrocyclic peptides by a remarkably facile ring-closing metathesis reaction. CD, IR, and ^{1}H NMR studies strongly suggest that peptides **3**, **4**, **7**, and **8** adopt predominantly 3_{10}-helical conformations in apolar organic solvent. Interestingly, while Karle's peptide **2** undergoes the subtle conformational shift from a 3_{10}- to an α-helix on going from $CDCl_3$ solution to the solid state, cyclic peptide **8** maintains a 3_{10}-helical conformation in both solution and in the crystal. The straightforward introduction of C−C bonds into peptides via RCM and the improved metabolic stability of these bonds[22] confirms olefin metathesis as an exceptional methodology for the synthesis of rigidified peptide architectures. Specifically, we believe the macrocyclization of small, hydrophobic peptide helices is uniquely suited to RCM in organic solvents because helical conformations are frequently favored in apolar media.

In view of the success of RCM as a route toward cyclic peptide helices, an attractive future application for RCM is in the synthesis of cyclic/tethered analogues of naturally occurring helical peptide antibiotics (e.g., the trichogin family of lipopeptaibols).[65] Another interesting application for olefin metathesis in the context of peptides is the syntheses of tethered peptide helix bundles and helix-turn-helix motifs by RCM, for potential use as peptide ligands for proteins and DNA.[66] The advent of water-soluble olefin metathesis catalysts has dramatically accelerated our pursuit toward such complex peptidic structures.[67] While almost all of our work with peptide RCM in organic solvents has relied on the preorganization of acyclic dienes through intramolecular H-bonding, RCM in water may require the strategic introduction of hydrophobic interactions[10] as a novel preorganizing factor. Water-soluble ruthenium carbenes[67]

(64) For the use of Aib-rich peptides containing (*i*) to (*i* + 3) lactam bridges as models of the 3_{10}-helix, see: Schievano, E.; Bisello, A.; Chorev, M.; Bisol, A.; Mammi, S.; Peggion, E. *J. Am. Chem. Soc.* **2001**, *123*, 2743−2751.

(65) (a) Toniolo, C.; Crisma, M.; Formaggio, F.; Peggion, C.; Monaco, V.; Goulard, C.; Rebuffat, S.; Bodo, B. *J. Am. Chem. Soc.* **1996**, *118*, 4952−4958. (b) Toniolo, C.; Peggion, C.; Crisma, M.; Formaggio, F.; Shui, X. Q.; Eggleston, D. S. *Nature Struct. Biol.* **1994**, *12*, 908−914. (c) Toniolo, C.; Benedetti, E. *Trends Biochem. Sci.* **1991**, *16*, 350−353.

(66) For a recent account of the de novo design of helix bundles, see: Hill, R. B.; Raleigh, D. P.; Lombardi, A.; DeGrado, W. F. *Acc. Chem. Res.* **2000**, *33*, 745−754.

(67) (a) Lynn, D. M.; Mohr, B.; Grubbs, R. H. *J. Am. Chem. Soc.* **1998**, *120*, 1627−1628. (a) Lynn, D. M.; Mohr, B.; Grubbs, R. H.; Henling, L. M.; Day, M. W. *J. Am. Chem. Soc.* **2000**, *122*, 6601−6609.

have been observed to be much more reactive toward internal olefins versus terminal olefins in aqueous-phase RCM reactions.[68] Therefore, the successful introduction of non-native *trans*-crotylglycine into expressed proteins via the manipulation of methionyl-tRNA synthetase specificity in *E. coli* has implications for performing olefin metathesis on complex, biologically relevant proteins in the future.[69]

Experimental Section

General Methods. NMR spectra were recorded on a JEOL GX-400, Bruker DPX 400 MHz, or Bruker AM-500 spectrometer. Chemical shifts are reported in parts per million (ppm) downfield from tetramethylsilane (TMS) with reference to internal solvent. Multiplicities are abbreviated as follows: singlet (s), doublet (d), triplet (t), quartet (q), and multiplet (m). Infrared spectra were obtained on a Perkin-Elmer 1600 Series FT-IR. Optical rotations were recorded on either a Jasco DIP-181 or DIP-1000 digital polarimeter at 589 nm and are reported as $[\alpha]_D$ (concentration (c) in grams/100 mL of solvent). Low- and high-resolution mass spectra were provided by the Southern California Mass Spectrometry Facility (University of California, Riverside). Analytical thin-layer chromatography (TLC) was performed using silica gel 60 F254 precoated plates (0.25 mm thickness) with a fluorescent indicator. Flash column chromatography was performed using silica gel 60 (230−400 mesh) from EM Science.[70] Alkylidene **1** was prepared according to published procedure.[13] RCM reactions were carried out under an argon atmosphere with dry, degassed solvents under anhydrous conditions.[71]

Peptide Synthesis. *N-tert*-Butyloxycarbonyl-*O*-allyl-L-serine and *N-tert*-butyloxycarbonyl-*O*-allyl-L-homoserine were prepared according to a modified literature procedure.[27] Peptides **3** and **4** were synthesized by conventional solution-phase synthesis methods using a racemization-free fragment condensation strategy.[28] Couplings were mediated by *N,N*-dicyclohexylcarbodiimide (DCC)/1-hydroxybenzotriazole (HOBT). The Boc group was used to protect the N-terminus, and the C-terminus was protected as a methyl ester. Deprotections were performed using 1:1 trifluoroacetic acid/CH_2Cl_2 and saponification, respectively. All intermediates were characterized by ^{1}H NMR (400 or 500 MHz) and TLC and, if necessary, purified by column chromatography on silica gel. Prior to the ring-closing metathesis (RCM) reaction, peptides **3** and **4** were purified by column chromatography on silica gel (83% EtOAc/hexane as eluent) and fully characterized (see below).

Circular Dichroism Studies. CD spectra were recorded on a JASCO J-600 spectropolarimater equipped with a JFC data processor (J-600 series spectropolarimater system software, Ver. 2.00) using 1 mm path length cuvettes. The scan speed was 5 nm/min, and spectra were averaged over 4 scans. Spectral baselines were obtained under analogous conditions as that for the samples. All spectra are baseline subtracted, converted to a uniform scale of molar ellipticity, and replotted. The temperature was maintained at 25 °C, and the sample concentration was 1.0 mM.

Acyclic Peptide (3). Heptapeptide **3** was prepared according to the standard solution phase protocol described in the general experimental above. ^{1}H NMR ($CDCl_3$, 500 MHz): δ 7.61 (1H, d, J = 8 Hz), 7.34 (1H, s), 7.32 (1H, d, J = 9 Hz), 7.30 (1H, d, J = 6 Hz), 7.05 (1H, d, J = 5 Hz), 6.78 (1H, d, J = 6 Hz), 5.87−5.77 (2H, br m), 5.23−5.06 (4H, br m), 4.95, (1H, apparent s), 4.73 (1H, m), 4.58 (1H, m), 4.24−4.16 (3H, br m), 3.97 (5H, m), 3.88−3.81 (4H, br m), 3.69 (3H, s), 2.23 (1H, m), 2.03 (1H, m), 1.71−1.38 (6H, br m), 1.50 (3H, s), 1.48 (3H, s), 1.46 (9H, s), 1.06 (3H, d, J = 7 Hz), 1.00 (6H, m), 0.93 (3H, d, J = 6 Hz), 0.88 (9H, d, J = 6 Hz), 0.86 (3H, d, J = 6 Hz). ^{13}C NMR ($CDCl_3$, 125 MHz): δ 175.9, 173.3, 173.2, 172.8, 171.8, 171.0, 170.2, 157.5, 134.8, 133.6, 117.6, 116.4, 80.9, 72.1, 71.9, 69.6, 62.4, 60.4, 56.9, 55.9, 54.4, 53.8, 51.9, 50.8, 40.4, 39.7, 29.5, 29.0, 28.2, 27.1, 24.4, 24.3, 23.2, 23.0, 22.8, 21.6, 21.0, 19.2, 19.0, 18.6, 17.1. IR (1.0 mM in $CHCl_3$, cm^{-1}): 3428, 3319, 2960, 2931, 2869, 1738, 1699, 1661, 1525, 1470, 1369, 1239, 1159, 1097. TLC: R_f = 0.26 (83% EtOAc/Hexane). $[\alpha]_D$ = −21.7 (c = 1.0, CH_2Cl_2). HRMS (FAB): calcd for $C_{44}H_{77}N_7O_{12}$ $[M + Na]^+$ 918.5528, found 918.5494.

Cyclic Peptide (7). To a solution of acyclic diene **3** (103 mg, 0.115 mmol) in 20 mL of $CHCl_3$ was added via syringe a solution of ruthenium alkylidene **1** (19 mg, 0.023 mmol) predissolved in 3 mL of $CHCl_3$. Within 10 min, the purple solution became orange-brown, and the solution was stirred an additional 4 h at 25 °C, when TLC analysis showed full disappearance of starting material. Triethylamine (1 mL) was added to the solution to deactivate any remaining catalyst, and the solution was concentrated to afford a brown, crystalline solid. Purification by column chromatography (4 cm × 12 cm silica gel, solvent gradient from 83% EtOAc/hexane to 100% EtOAc) afforded 85 mg (85%) of cyclic olefin isomers **5** as an off-white powder. Cyclic peptides **5** (20 mg, 0.023 mmol) were then dissolved in 2.9 mL of anhydrous EtOH, and 10% Pd−C (8 mg, 0.4 wt/wt) was added to the stirring solution. The system was purged with hydrogen, and allowed to stir under 1 atm of hydrogen for 2 h. The solution was then filtered (2×) through a pad of Celite and concentrated to afford 19.6 mg (98%) of hydrogenated macrocycle **7** as a white, crystalline solid. ^{1}H NMR (500 MHz, $CDCl_3$): δ 7.55 (2H, two amide NHs obscured, apparent m), 7.49 (1H, d, J = 7 Hz), 7.33 (1H, br d), 7.04 (1H, br d), 6.80 (1H, s), 5.07 (1H, br d), 4.72 (1H, m), 4.53 (1H, m), 4.46 (1H, m), 4.31 (1H, m), 4.11 (1H, m), 4.01 (1H, m), 3.93 (1H, m), 3.88 (1H, m), 3.72 (1H, m), 3.70 (3H, s), 3.59 (1H, m), 3.51 (2H, m), 3.43 (1H, m), 3.40 (1H, m), 3.25 (1H, m), 2.43 (1H, m), 2.26 (1H, m), 1.95−1.33 (6H, m), 1.68 (4H, d, J = 6 Hz), 1.48 (3H, s), 1.47 (3H, s), 1.46 (9H, s), 1.05 (4H, d, J = 7 Hz), 0.94 (12H, m), 0.89 (8H, m). ^{13}C NMR (125 MHz, $CDCl_3$): δ 175.1, 172.9, 172.5, 172.1, 170.4, 157.1, 81.1, 71.1, 71.0, 70.2, 68.5, 61.6, 59.5, 57.3, 55.5, 55.1, 54.7, 52.2, 51.7, 40.4, 30.2, 29.9, 28.3, 27.5, 25.8, 25.4, 24.7, 23.6, 23.0, 22.8, 22.2, 22.1, 19.7, 19.5, 18.1, 18.0. IR (1.0 mM in $CHCl_3$, cm^{-1}): 3431, 3331, 2960, 2931, 2869, 1737, 1663, 1530, 1465, 1367, 1240, 1160, 1099, 1029. TLC: R_f = 0.10 (83% EtOAc/hexane). $[\alpha]_D$ = +2.06 (c = 1.0, CH_2Cl_2). HRMS (FAB): calcd for $C_{42}H_{75}N_7O_{12}$ $[M + Na]^+$ 892.5371, found 892.5361.

Acyclic Peptide (4). Heptapeptide **4** was prepared according to the standard solution-phase protocol described in the general experimental above. ^{1}H NMR ($CDCl_3$, 500 MHz): δ 8.11 (1H, d, J = 3 Hz), 7.62 (1H, d, J = 8 Hz), 7.55 (1H, s), 7.35 (1H, d, J = 6 Hz), 7.22 (1H, d, J = 8 Hz), 6.79 (1H, d, J = 8 Hz), 5.94−5.82 (2H, br m), 5.33−5.06 (4H, br m), 4.85 (1H, d, J = 2 Hz), 4.55 (2H, m), 4.22 (3H, m), 4.10 (1H, m), 3.97 (2H, m), 3.91 (2H, m), 3.76 (1H, m), 3.68 (3H, s), 3.66 (1H, m), 3.54 (2H, m), 2.50 (1H, m), 2.36 (1H, m), 2.15 (2H, m), 2.01 (2H, m), 1.70−1.35 (6H, br m), 1.50 (3H, s), 1.48 (12H, apparent s), 1.04−0.87 (24H, br m). ^{13}C NMR (125 MHz, $CDCl_3$): δ 186.6, 176.0, 173.4, 173.2, 172.9, 172.4, 171.7, 157.4, 135.4, 134.2, 117.7, 116.5, 81.6, 72.5, 71.8, 69.0, 67.4, 62.38, 62.37, 62.3, 60.2, 57.3, 56.2, 54.3, 52.1, 51.2, 51.1, 40.9, 40.2, 31.3, 30.6, 29.8, 29.1, 28.4, 27.4, 25.0, 24.8, 23.5, 23.1, 23.0, 21.9, 21.6, 19.5, 19.3, 18.3, 17.3. IR (1.0 mM in $CHCl_3$, cm^{-1}): 3439, 3326, 3005, 2962, 2933, 2872, 1742, 1701, 1666, 1525, 1488, 1368, 1283, 1227, 1159, 1100. TLC: R_f = 0.39 (83% EtOAc/hexane). $[\alpha]_D$ = −20.9 (c =1.0, CH_2Cl_2). HRMS (FAB): calcd for $C_{46}H_{81}N_7O_{12}$ $[M + H]^+$ 924.6021, found 924.6055.

Cyclic Peptide (8). To a solution of acyclic diene **4** (1.00 g, 1.08 mmol) in 200 mL of $CHCl_3$ was added via syringe a solution of ruthenium alkylidene **1** (178 mg, 0.216 mmol) predissolved in 16 mL of $CHCl_3$. Within 10 min, the purple solution became orange-brown, and the solution was stirred

(68) Kirkland, T. A.; Lynn, D. M.; Grubbs, R. H. *J. Org. Chem.* **1998**, *63*, 9904−9909.

(69) Kiick, K. L.; van Hest, J. C. M.; Tirrell, D. A. *Angew. Chem., Int. Ed.* **2000**, *39*, 2148−2152.

(70) Still, W. C.; Kahn, M.; Mitra, A. *J. Org. Chem.* **1978**, *43*, 2923−2925.

(71) CH_2Cl_2 was purified by passage through a solvent column composed of activated alumina (A-2) and supported copper redox catalyst (Q-5 reactant). See: Pangborn, A. B.; Giardello, M. A.; Grubbs, R. H.; Rosen, R. K.; Timmers, F. J. *Organometallics* **1996**, *15*, 1518−1520.

for an additional 3 h at 25 °C, when TLC analysis showed full disappearance of starting material. Triethylamine (3 mL) was added to the solution to deactivate any remaining catalyst, and the solution was concentrated to afford a brown, crystalline solid. Purification by column chromatography (5 cm × 15 cm silica gel, solvent gradient from 75% EtOAc/Hexane to 100% EtOAc) afforded 869 mg (90%) of cyclic olefin isomers **6** as an off-white powder. Cyclic peptides **6** (676 mg, 0.756 mmol) were then dissolved in 92 mL of anhydrous EtOH, and 10% Pd−C (270 mg, 0.4 wt/wt) was added to the stirring solution. The system was purged with hydrogen, and allowed to stir under 1 atm of hydrogen for 2 h. The solution was then filtered (2×) through a pad of Celite and concentrated to afford 661 mg (98%) of hydrogenated macrocycle **8** as a white, crystalline solid. ^{1}H NMR (CD_2Cl_2, 400 MHz): δ 7.54 (1H, d, J = 8 Hz), 7.47 (1H, s), 7.23 (1H, d, J = 4 Hz), 7.09 (1H, d, J = 8 Hz), 7.03 (1H, d, J = 8 Hz), 6.74 (1H, d, J = 4 Hz), 5.17 (1H, apparent s), 4.46 (1H, m), 4.25 (1H, m), 4.17 (2H, m), 3.97 (1H, m), 3.80 (1H, m), 3.67 (3H, br s), 3.53−3.22 (8H, br m), 2.43 (1H, m), 2.33 (1H, m), 2.15 (2H, m), 1.72 (2H, m), 1.63−1.30 (10H, br m), 1.47 (12H, apparent s), 1.45 (3H, s), 1.10−0.85 (24H, br m). ^{13}C NMR ($CDCl_3$, 125 MHz): δ 176.5, 174.2, 173.6, 173.4, 172.9, 172.6, 172.5, 157.5, 80.9, 71.2, 70.6, 68.1, 66.3, 62.7, 60.4, 57.0, 55.3, 54.4, 52.34, 52.29, 51.1, 40.72, 40.68, 31.9, 31.2, 29.8, 29.1, 28.5, 27.5, 26.6, 25.8, 25.0, 24.7, 23.4, 23.1, 22.8, 22.3, 21.7, 19.7, 19.4, 18.9, 18.0. IR (1.0 mM in $CHCl_3$, cm^{-1}): 3427, 3324, 3001, 2960, 2935, 2871, 1736, 1698, 1665, 1602, 1528, 1369, 1275, 1235, 1157, 1105. TLC: R_f = 0.10 (83% EtOAc/hexane). $[\alpha]_D = -2.09$ (c = 1.0, CH_2Cl_2). HRMS (FAB): calcd for $C_{44}H_{79}N_7O_{12}$ $[M + H]^+$ 898.5865, found 898.5893.

Acknowledgment. Work at Caltech was generously supported by the National Institutes of Health (NIH) and AstraZeneca. Work at Pomona College was supported by the National Science Foundation (NSF). H.E.B. thanks the ACS Division of Organic Chemistry for a predoctoral graduate fellowship (supported by Pfizer, Inc.). Dr. Saeed Khan (UCLA) is gratefully acknowledged for X-ray crystallographic analyses. Prof. Andrew T. Morehead, Jr. is acknowledged for assistance in preliminary molecular modeling studies. We thank Dr. Isabella L. Karle, Prof. Barbara Imperiali, Prof. Scott J. Miller, and Dr. Keith Russell for helpful discussions. We are grateful to Jack Sadowsky for his creative artwork featured on the cover of this journal.

Supporting Information Available: Tables of experimental data, distances, angles, torsion angles, stereoview plots, unit cell plots, and position and displacement parameters for cyclic peptide **8**. Full NMR assignments for peptides **4** and **8** in CD_2Cl_2, tables of interproton distance restraints, Ramachandran maps, and SYBYL mol2 files of the calculated structures. This material is available free of charge via the Internet at http://pubs.acs.org.

JO015533K